Behaviour and mechanisms of molecular vibrations induced by a pulsed voltage in a silicone elastomer used for device encapsulation

Junyu Wei, Dongxin He, Teng Gao, Lin Zhu, Haochen Wang, Qingquan Li, G. Teyssedre

Received: 10 March 2023 | Revised: 3 May 2023 | Accepted: 23 May 2023

High Voltage

DOI: 10.1049/hve2.12363

ORIGINAL RESEARCH

Behaviour and mechanisms of molecular vibrations induced by a pulsed voltage in a silicone elastomer used for device encapsulation

Junyu Wei[1] | Dongxin He[1] | Teng Gao[1] | Lin Zhu[2] | Haochen Wang[1] | Qingquan Li[1] | Gilbert Teyssedre[3]

[1]Shandong Provincial Key Laboratory of UHV Transmission Technology and Equipment School of Electrical Engineering, Shandong University, Jinan, China

[2]School of Materials Science and Engineering, Shandong University, Jinan, China

[3]UPS, INPT, CNRS, LAPLACE (Laboratoire Plasma et Conversion d'Energie), University of Toulouse, Toulouse, France

Correspondence

Dongxin He, Shandong Provincial Key Laboratory of UHV Transmission Technology and Equipment School of Electrical Engineering, Shandong University, Jinan 250061, China.
Email: hdx@sdu.edu.cn

Associate Editor: Jin Li

Funding information

National Natural Science Foundation of China, Grant/Award Numbers: 51907105, 52277155

Abstract

Silicone elastomers are widely used to encapsulate power electronic devices. However, such devices may be subjected to square-wave pulsed voltages with a high rate of change, which can create significant challenges for encapsulation insulation. In this article, the molecular vibration of silicon elastomer at the edge of pulsed electric field is studied. Firstly, the relationship between the intensity of molecular vibration and the parameters of pulsed electric field is explored. The experimental results show that the amplitude of the vibrations decreases as the pulse-edge time increases, and it increases linearly as the pulse-edge slope increases. Furthermore, the amplitude of the vibrations is proportional to the square of the amplitude of the pulsed electric field, and it increases as the space charge density increases. Then, the force analysis of charged molecule at the pulse edges is calculated, and the theoretical change law of molecular vibration intensity with pulse edge slope is deduced. Comparing the theoretical results with the experimental results, it is found that they are highly consistent. Finally, electrically induced mechanical stress caused by molecular vibration was shown to be an important factor in insulation failure.

1 | INTRODUCTION

High-voltage power electronic devices, such as insulated-gate bipolar transistors (IGBTs) and metal–oxide–semiconductor field-effect transistors (MOSFETs) benefit from a high power density, small size, and convenient operation; hence, they are widely used in modern power systems in applications such as direct-current (DC) transmissions and energy-grid connections [1, 2]. Silicone elastomers are good insulators and, once cured, they are suitably elastic and viscose to support and bond to the internal structures of electronic devices. Therefore, they are used in the packaging structures of high-voltage power electronic devices [3–5].

Insulators are more likely to deteriorate under pulsed electric fields than they are under DC or alternating-current (AC) electric fields with the same amplitude and frequency. This is because, under a pulsed voltage, the initial voltage required to initiate electrical treeing is lower [6] and partial discharges are more intense [7], which increases the probability that the insulator will fail. An important characteristic of pulsed voltages is the sudden change in the voltage amplitude at the pulse edges. Research has shown that the average life of an insulator decreases significantly as the rise time of a pulse decreases [8]. Therefore, researchers have speculated that sharp increases and decreases in the voltage at pulse edges may adversely affect insulators [9–11].

Following the development of wide-bandgap semiconductor materials such as silicon carbide (SiC) and gallium nitride, it has become necessary for power electronic devices and equipment to withstand pulsed voltages with higher frequencies and steeper slopes. For example, a photoconductive switch based on SiC utilises a pulsed voltage of 74.5 kV and a turn-on rise time of 2.05 ns [12], and high-voltage silicon carbide IGBTs have maximum voltage-repetition frequencies between 100 kHz and the megahertz range with voltage-rise rates up to hundreds of kV/μs [13]. Therefore, to improve the reliability of high-voltage power electronic devices, it is important to explore the mechanisms of insulation deterioration under pulsed voltages with high amplitudes, repetition rates, and change rates.

Insulation degradation under pulsed electric fields is affected by the strength of the electric field and the application mode, which may be closely related to the unique response mechanism of the space charge in the medium [14–18]. Space charges accumulate at defects in insulator materials and their unique behaviour is triggered by pulsed electric fields. Thus, further damage to the molecular structure occurs at the defect site and electrical treeing is initiated [19, 20]. Literatures [21–23] have studied the initiation mechanism of electrical treeing under a pulsed electric field. It is believed that the charge is injected into the material under the action of the pulsed voltage. Subsequently, it collides with the molecular chain, or interacts with the surrounding molecular chain in the form of electromagnetic waves, thereby destroying the microstructure of the insulating material and leading to electrical treeing. Literature [24, 25] investigated the effect of pulse parameters on space charge. It is found that negative electric field with higher frequency and positive electric field with lower frequency can accelerate the insulation sample's space-charge accumulation. The above research speculates on the behaviour of the space charge under a pulsed electric field from the macroscopic failure phenomenon, and the research results can be used as a reference.

Electrically induced mechanical stress also affects the deterioration of insulators. In one study, Ren et al. found that a nanosecond-pulsed electric field produced mechanical stress perpendicular to the electric field, which caused the insulating material to crack [26]. In addition, the basic principle of the pulsed electroacoustic (PEA) method shows that a narrow pulsed electric field with steep edges can excite the space charge and cause the molecular chain to vibrate [27]. The frequency component at the edge of a nanosecond pulse is similar to the frequency component of a pulse applied as part of the PEA method. Therefore, the high-frequency alternating stress caused by molecular vibrations at the edges of nanosecond pulses may also contribute to insulation degradation. This phenomenon was also established in a recent preliminary study by Zhang et al. [28]. They found that, when a square-wave pulsed electric field with an edge time of 50 ns to 200 μs was applied to a polyimide sample, there was a strong acoustic signal near the pulse edge. According to the time delay calculation, the sound originated inside the material; therefore, it is believed that it was caused by the molecular vibrations that occurred when the electric charge within the material was excited. However, this study only involved a preliminary analysis of this phenomenon and it did not consider the effects of charge accumulation on the molecular vibrations; consequently, it did not include a theoretical derivation.

Molecular vibrations induced by a pulsed electric field may adversely affect the encapsulation of a device. Therefore, it is necessary to understand the molecular behaviour of insulator materials such as silicone elastomers under square-wave pulsed electric fields to establish their deterioration mechanisms. This study considered a silicone elastomer as the research object. First, the variations in the electroacoustic signals generated by molecular vibrations under various pulsed electric fields with different space charge densities were investigated. Second, a dynamic model of the charged molecules at the pulse edges was established. Third, the force of the charged molecules at the pulse edges was analysed, and the trends in the amplitude of the molecular vibrations under pulsed electric fields with different edge slopes were analysed. Hence, this research can be used to improve the preparation of insulating materials used to encapsulate high-voltage power electronic devices.

2 | EXPERIMENTAL SETUP

2.1 | Sample selection and preparation

The silicone elastomer used in this experiment was Dow Corning SYLGARD 184. The elastomer base and curing agent were fully mixed at a weight ratio of 10:1 and then injected into a mould (length × width × thickness: 50 × 50 × 0.8 mm). The mould was placed into a constant-pressure chamber for degassing, which removed any gas from the mixture and prevented bubbles that could affect the experimental results. After degassing, the mixture was put in a vacuum oven and cured for 2 h at 80°C to obtain a transparent elastomer with high toughness.

2.2 | Experimental device

In this study, a method of simultaneously monitoring the molecular vibrations and charge distribution was developed. The experimental setup is shown in Figure 1a. A DC power supply was used to apply a voltage with a high field strength to the sample, which accelerated the accumulation of the space charge in the sample. A square-wave pulsed power supply produced a square-wave pulsed voltage with an edge time ranging from a few nanoseconds to microseconds (as shown in Figure 4). The pulse generator was triggered by a short square-wave signal from the trigger control circuit and continuously output a pulsed voltage with a rise time of 5 ns. As shown in Figure 1b, the molecular-vibration test unit consisted of a high-voltage electrode, semiconducting layer, grounding electrode, polyvinylidene fluoride (PVDF) sensor, and amplifier. It converted the acoustic signals generated by the molecular vibrations into electrical signals. A semiconducting layer was placed

between the sample and the high-voltage electrode to improve the electric field distribution around the high-voltage electrode and to prevent flashover.

A negative square-wave pulsed voltage with a frequency of 500 Hz and duty cycle of 50% (as shown in Figure 2) was applied to the sample and the electroacoustic signal generated by the molecules vibrating under the electric field was recorded. The variations in the amplitudes of the electroacoustic signals were investigated using pulses with different edge times and amplitudes. In addition, the space charge density was varied by applying a DC voltage for different durations to explore the effect of the space charge density on the molecular-vibration waveform. Finally, the experimental rules were summarised to provide a basis for analysing the behaviour of the electric charge at the edge of a pulse.

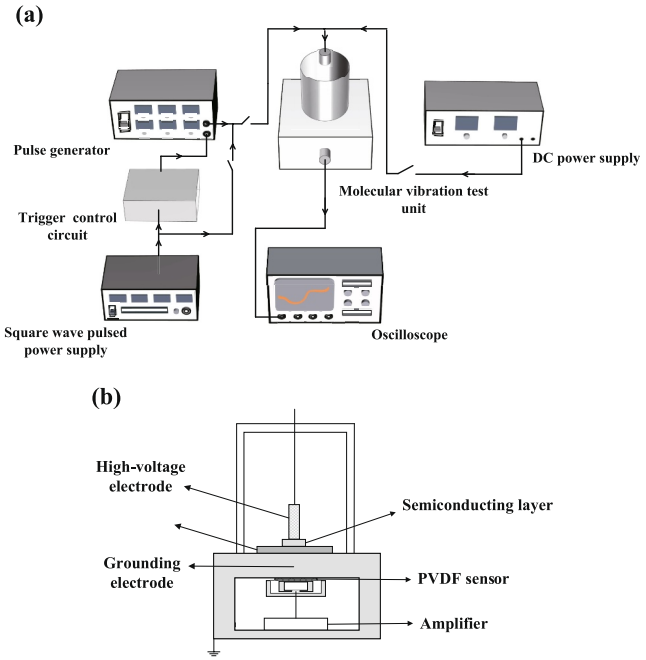

FIGURE 1 Monitoring platform used to simultaneously monitor molecular vibrations and the charge distribution. (a) Schematic of the test platform and (b) the molecular-vibration test unit.

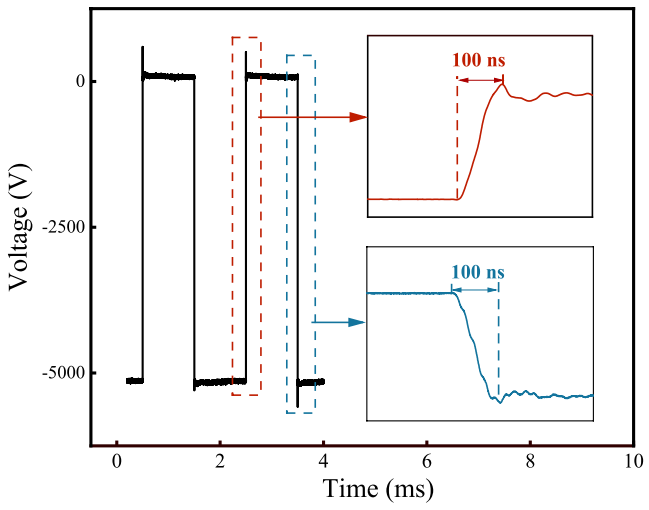

FIGURE 2 Waveform of the square-wave pulsed voltage and its edge.

3 | EXPERIMENTAL RESULTS

3.1 | Electroacoustic signal at the pulse edge

A square-wave pulsed electric field with an amplitude of 5 kV and a rise time of 100 ns was applied to the sample. The interval between the rising edge of the pulsed electric field and the electroacoustic signal detected by the PVDF sensor is shown in Figure 3a. It is noted that no pulse electric field is applied, and the electroacoustic signal is only generated under the excitation of the edge of the square wave pulse electric field. Owing to the structure of the molecular-vibration test unit (shown in Figure 1b), the electroacoustic signal generated by molecular vibrations in the silicone elastomer passed through the aluminium plate before reaching the PVDF sensor, which resulted in a delay between the molecular-vibration signal and the pulse edge. Based on the

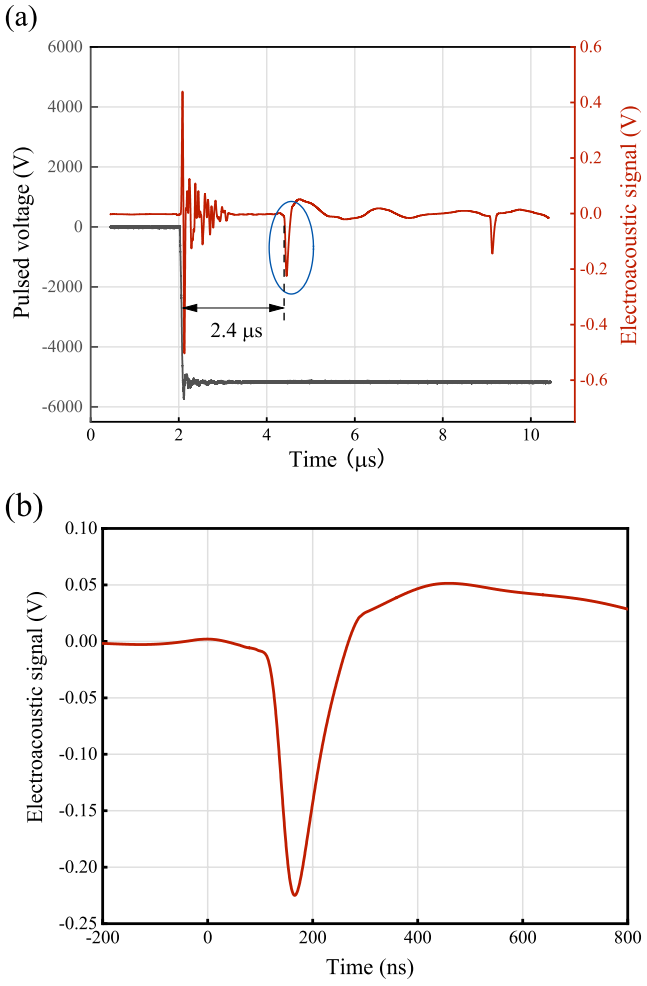

FIGURE 3 (a) Relationship between the timings of the pulse edge and electroacoustic signal and (b) waveform of the electroacoustic signal.

calculations, the time delay was determined to be 2.4 μs, which is the same as the delay between the electroacoustic signal and the pulse application, as shown in Figure 3b. Therefore, it can be concluded that the marked region was caused by molecular vibrations in the sample. The effects of the pulse parameters and space charge density on the waveform of the electroacoustic signal are discussed in subsequent subsections.

3.2 | Effects of pulse parameters on the amplitude of the electroacoustic signal

3.2.1 | Pulse-edge rise time

The rise time (the rate of change at the rising pulse edge) of the pulsed electric field was varied and the electroacoustic signals were recorded, as shown in Figure 4. T_r represents the rise time of pulsed voltage. As the rise time increased, the amplitude of the peak electroacoustic signal gradually decreased. At rise times of 100 and 400 ns, vibration peaks were apparent. However, when the rise time increased to 1 μs, the amplitude of the vibration peak decreased and the width of the peak increased. Moreover, when the rise time reached 50 μs, the electroacoustic signal was approximately straight and the peak was negligible. This indicates that the amplitude of the molecular vibrations induced by a pulsed electric field is affected by the rise time. Therefore, substantial molecular vibrations can only be observed under pulsed electric fields with rise times in the nanosecond range.

The peak value of the electroacoustic signal reflects the amplitude of the molecular vibrations, as shown in Figure 5. The amplitude of the molecular vibrations decreased sharply as the rise time increased. In the nanosecond range, the molecular vibrations were extremely intense; however, the amplitude decreased sharply at 1–10 μs, and the vibrations were significantly reduced in the microsecond range. When the rise time was greater than 50 μs, the molecules hardly vibrated. Therefore, the amplitude of molecular vibrations is affected by the rise time.

3.2.2 | Maximum slope at the pulse edge

The most prominent feature of pulse edges is a sudden change in the voltage amplitude, which can be determined from the slope. Figure 6a shows the slopes corresponding to different positions along the pulse edge. The amplitude of the voltage at the pulse edge does not change linearly; instead, it changes rapidly at first and then the rate of change decreases as it approaches the steady-state value. As the voltage changes along the pulse edge, there must be a position where the slope is largest, that is, where the excitation of charged molecules is greatest. The maximum slope occurs near the start of the pulse edge; therefore, the slope at the start of the pulse edge is the most critical factor affecting the amplitude of the molecular vibrations.

The maximum slopes corresponding to different rise times were compared to the amplitudes of the molecular vibrations, as shown in Figure 6b. This indicates that the vibration amplitude increases linearly as the maximum slope at the pulse edge increases.

3.2.3 | Amplitude of the pulsed voltage

The relationship between the amplitudes of the molecular vibrations and the pulsed voltage was investigated by varying the voltage from 2000 to 5000 V at a fixed edge time of 100 ns; the results are shown in Figure 7. The relationship between the amplitudes of the molecular vibrations and the pulsed voltage was approximately square. This is because the amplitude of the electric field is affected by both the density and behaviour of the polarised charge. As the amplitude of the electric field increased, the charges generated at the surface of the material

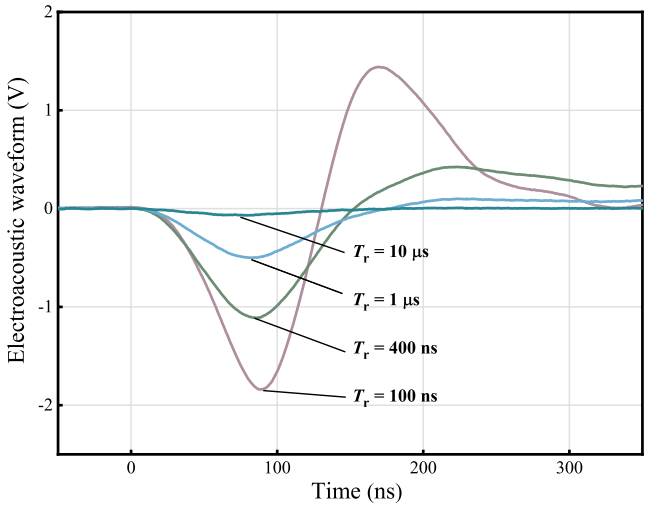

FIGURE 4 Waveforms of electroacoustic signals with different rise times.

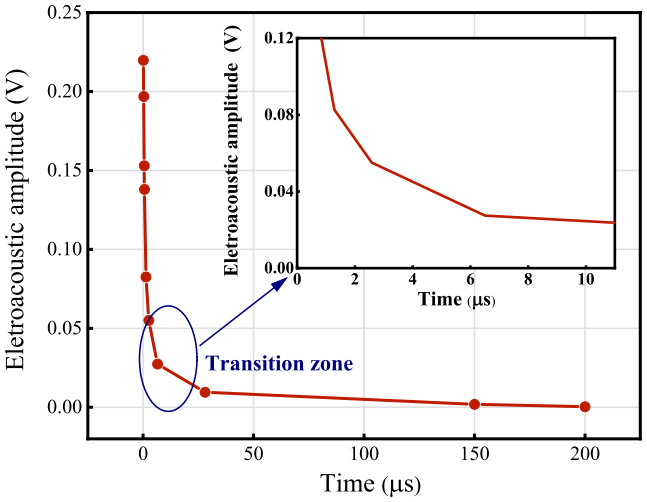

FIGURE 5 Variations in the molecular vibrations with different rise times.

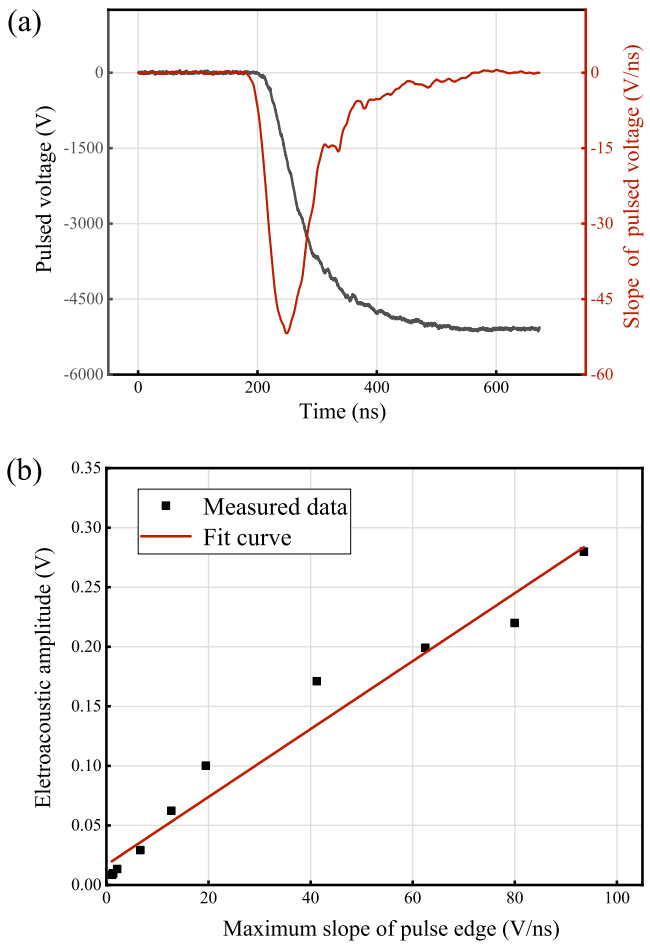

FIGURE 6 (a) Edge slope of the pulsed voltage and (b) amplitude of the molecular vibrations against the maximum edge slope.

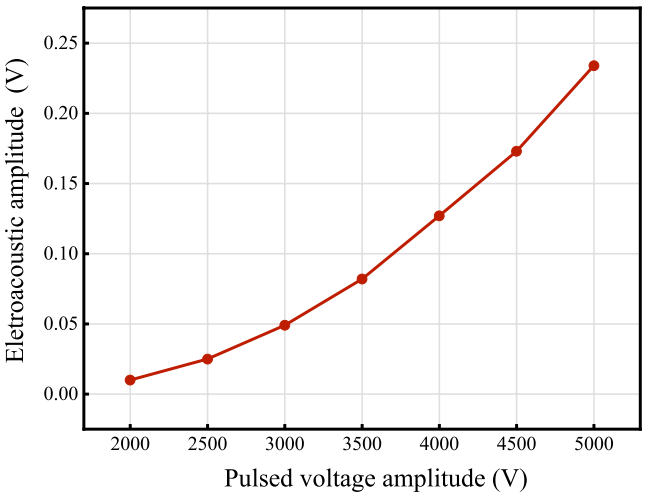

FIGURE 7 Amplitude of the molecular vibrations against the amplitude of the pulsed voltage.

became more polarised. Increasing the electric field amplitude at a fixed edge time increases the slope of the edges; hence, the charge-excitation effect increases. Therefore, the amplitude of molecular vibrations is proportional to the square of the amplitude of the pulsed voltage.

3.3 | Effects of space charge density on the amplitude of the electroacoustic signal

The relationship between the electroacoustic signal and the space charge density was investigated. First, a square-wave pulsed voltage with an amplitude of 5 kV, edge time of 100 ns, and frequency of 500 Hz was applied to the sample. The electroacoustic signal was measured when there was no space charge accumulated in the sample, and this signal was used as the reference signal. Subsequently, a high-amplitude DC electric field was applied to the sample to accelerate the accumulation of space charge in the silicone elastomer. The DC voltage amplitude was −8 kV, the sample was 800 μm thick, and the corresponding field strength was −10 kV/mm. At specific intervals, the DC voltage was turned off and a square-wave pulsed voltage was applied; thus, the effects of space charge accumulation on the electroacoustic waveform were investigated.

The waveform of the electroacoustic signal during charge accumulation is shown in Figure 8. When the voltage-application time was 0 min, that is, when there was no space charge in the sample, there was only one negative peak in the electroacoustic signal. This peak was generated by molecular vibrations driven by the interface charge. When the voltage was applied for 10 min, a positive-polarity peak (marked by a circle) was observed to the right of the negative-polarity peak. Up to 60 min, as the voltage-application time increased, the amplitudes of the positive- and negative-polarity peaks increased. After 60 min, as the voltage-application time increased, the amplitudes of the positive- and negative-polarity peaks decreased.

A positive-polarity peak was formed by the molecular vibrations caused by the heteropolar charge that accumulated near the interface. Owing to incomplete crosslinking, impurities formed during the preparation of the silicone elastomer. Under an electric field, these impurities ionised and migrated in the direction of the corresponding electrode, which formed a heteropolar charge. However, homopolar charges were induced at the interface. The interface and space charges had opposite polarities; hence, they moved in opposite directions under the electric field. Therefore, two peaks with opposite polarities were observed on the oscilloscope.

When the voltage-application time was less than 60 min, the densities of the heteropolar charges near the interface and the homopolar charges at the interface increased as the application time increased. Therefore, the amplitudes of the two peaks also increased as the application time increased. When the voltage-application time exceeded 60 min, the electrode began to inject the same polar charge. The injected homopolar charges and previously accumulated heteropolar charges cancelled each other out, which reduced the density of the charges at the interface and the space charges. Therefore, the amplitudes of the two peaks of the electroacoustic signal decreased as the application time increased.

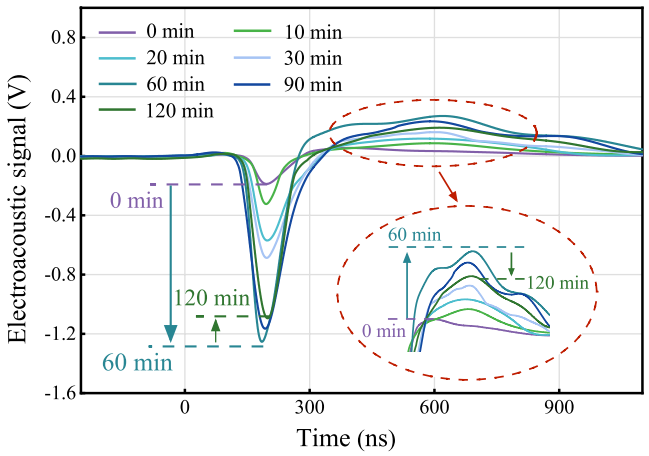

FIGURE 8 Wave-form of the electroacoustic signal after a DC voltage was applied for different durations.

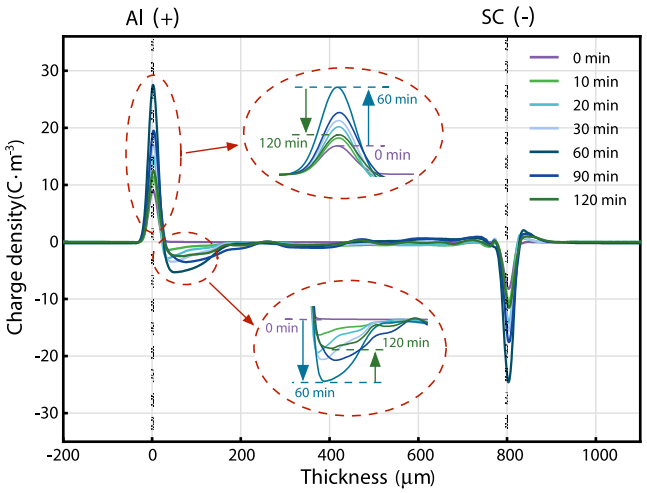

FIGURE 9 Space charge density against the voltage-application time.

To verify this conjecture, a DC voltage with an amplitude of −8 kV was applied to the sample, and the variation in the space charge distribution over time was investigated, as shown in Figure 9. When the voltage-application time was less than 60 min, the interface charge density increased as the application time increased, and heteropolar charges accumulated near the interface. When the voltage-application time was greater than 60 min, the interface charge density decreased as the application time increased, and the heteropolar charge density near the interface decreased. This indicates that homopolar charge injection occurred near the interface and that the growth rate of the homopolar charge was greater than that of the heteropolar charge. However, the total heteropolar charge was still greater than the total homopolar charge.

Comparing Figures 8 and 9 shows that the changes in the negative and positive peak amplitudes of the electroacoustic signal were consistent with the changes in the interface charge and space charge in the sample. This indicates that the electroacoustic signal, detected by the PVDF sensor, was generated by charge-driven molecular vibration and that the amplitude of the molecular vibrations increased as the space charge density increased.

4 | MOLECULAR-VIBRATION MECHANISMS AT THE PULSE EDGE

The experimental results showed that the polarisation charge at the sample interface and the internal space charge drive molecular vibrations under the excitation of the pulse edge. Moreover, the amplitude of the vibrations was mainly affected by the slope of the pulse edge. Therefore, the charge behaviour at the pulse edge was analysed dynamically to determine the mathematical relationship between the vibration amplitude of the charged molecules and the slope of the pulse edge. Subsequently, the theoretical results were compared with experimental results to verify their accuracy.

4.1 | Problems with the electroacoustic equation

According to the principle of the PEA method, there is a correlation between the peak of the electroacoustic signal and the distribution of the space charge. Takata et al. [29] deduced the relationship between the space charge density and the electroacoustic signal peak under Gaussian-pulse excitation. However, in this study, the excitation signal was not a Gaussian pulse but the edge of a pulsed electric field, which can be represented by a slope-step function. The effect of the signal on the charged molecules is not instantaneous; therefore, the electroacoustic signal cannot be regarded as the propagation of the excitation source. In addition, derivations in the literature show that the peak value of the acoustic wave is only dependent on the space charge density and the amplitude of the Gaussian pulse [29]. However, the experimental results showed that when the excitation signal was a slope-step function, the peak value of the acoustic wave was dependent on the maximum slope at the edge of the pulse. This is also beyond the interpretation of traditional electroacoustic equations. Therefore, the correlation between the amplitude of the vibrations and the maximum slope at the pulse edge must be studied dynamically.

4.2 | Wave equation under slope-step excitation

The fundamental wavelength of the sound wave is significantly smaller than the diameter of the detection electrode; therefore, the space charge distribution and the propagation of the sound wave are considered to be constant on the plane perpendicular to the electric field and that they only change in the direction parallel to the electric field. In other words, the propagation of sound waves can be approximated using a one-dimensional transmission model. The wave equation for the propagation of sound waves can be expressed as follows:

$$\frac{\partial^2 u}{\partial t^2} = v_s^2 \frac{\partial^2 u}{\partial x^2} + E(x,t) \cdot \rho(x), \tag{1}$$

where v_s is the propagation speed of sound waves, u is the displacement of the particle from its equilibrium position, $E(x,t)$ is the applied electric field, and $\rho(x)$ is the density distribution function of the space charge. Thus, $E(x,t)\cdot\rho(x)$ is the electric field force. Equation (1) is a non-homogeneous second-order partial differential equation. Because the space charge density distribution function $\rho(x)$ is unknown, it is difficult to obtain an analytical solution. Therefore, other methods must be used to obtain an expression for the acoustic signals generated by molecular vibrations under a given excitation.

A wave is the propagation of vibrations in a continuous medium. When a particle is disturbed, it vibrates near the equilibrium position. Owing to the forces between adjacent particles, when one particle vibrates it causes adjacent particles to vibrate as well. In other words, vibrations propagate through a continuous medium. It is generally believed that the interactions between particles are elastic and that the magnitude of the force is proportional to the displacement from the equilibrium position. Therefore, the wave equation can be transformed into a vibration equation. Furthermore, a force analysis was performed for charged molecules at a single position, which provided a vibration equation for charged molecules under slope-step excitation. Thus, the corresponding relationship between the vibration amplitude and the slope of the excitation was deduced.

4.3 | Vibration equation for charged molecules

Owing to the strong coupling between electrons and molecules, acoustic signals are generated by charge-driving molecular vibrations. Molecules are affected by a variety of complex forces as they move, such as those exerted by other molecules, the viscosity of the material, and the electromagnetic force of the internal charge. There are no exact expressions for most of these forces; therefore, it is difficult to obtain a specific expression for the vibration of charged molecules under an electric field. However, the effects of sudden changes in the electric field force at the pulse edge are a form of unsteady excitation, and the response of the system is also unsteady. The solutions to vibration problems caused by sudden impacts are usually focused on the maximum value of the system during the unsteady response and they do not require accurate solutions. Therefore, the vibration model was simplified accordingly.

The internal microforce is equivalent to the elastic restoring force and resistance. Under an impact, the system quickly reaches the maximum vibration amplitude. Moreover, the damping force is insufficient to dissipate the large amount of mechanical energy; therefore, damping effects were disregarded. Furthermore, the key factor was the peak amplitude of the vibrations; therefore, the details of the vibration process were not considered. Hence, only the first-order elastic restoring force was considered in the analysis and the elastic coefficient was regarded as a constant. The simplified force during the vibration of the charged molecules is shown in Figure 10. Notably, the spring-oscillator model was used in the derivation of the one-dimensional wave equation presented in Equation (1). However, only the effect of the elastic force between adjacent particles was considered, whereas the effect of resistance was disregarded. The particles vibrate under the joint action of elastic and external forces, which completes the wave equation. Therefore, the model and the simplified process used in this study were sufficiently reasonable.

The forces on the charged molecules at the rising and falling edges of the pulsed electric field are similar; therefore, only the force at the rising edge was analysed. According to force analysis, the dynamic equation of charge movement can be expressed as follows:

$$m\ddot{x} + cx = qE(t), \tag{2}$$

where m is the molecular mass, c is the elastic recovery coefficient, and $qE(t)$ is the electric field force. The electric field generated by the charged molecules is shown in Figure 11. Its size does not depend on its molecular position, only the time. Thus, it can be expressed as follows:

$$E(t) = \begin{cases} kt, & 0 \le t < \dfrac{E_0}{k} \\ E_0, & t > \dfrac{E_0}{k} \end{cases}, \tag{3}$$

where k is the slope of the rising edge of the electric field and E_0 is the amplitude of the electric field.

Solving Equation (3) gives an expression for the molecular vibrations, that is,

$$\begin{aligned} x(t) = \frac{kX_0}{p} \Bigg\{ & (pt - \sin pt)u(t) \\ & - \left[p\left(t - \frac{E_0}{k}\right) - \sin p\left(t - \frac{E_0}{k}\right) \right] u\left(t - \frac{E_0}{k}\right) \Bigg\}. \end{aligned} \tag{4}$$

Here, parameters p and X_0 are defined as $p^2 = c/m$ and $X_0 = E_0 q/c$, respectively, and $u(t)$ is the unit-step function.

According to the definition of the step function, Equation (4) can be rewritten as follows:

$$x(t) = \begin{cases} X_0\left(kt - \dfrac{k}{p}\sin pt\right) & 0 < t \le \dfrac{E_0}{k} \\ X_0\left[E_0 - \dfrac{k}{p}\sin pt + \dfrac{k}{p}\sin p\left(t - \dfrac{E_0}{k}\right)\right] & t > \dfrac{E_0}{k} \end{cases} \tag{5}$$

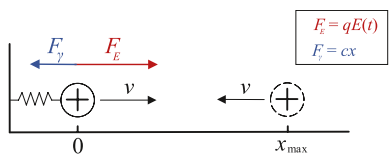

FIGURE 10 Simplified molecular-vibration model.

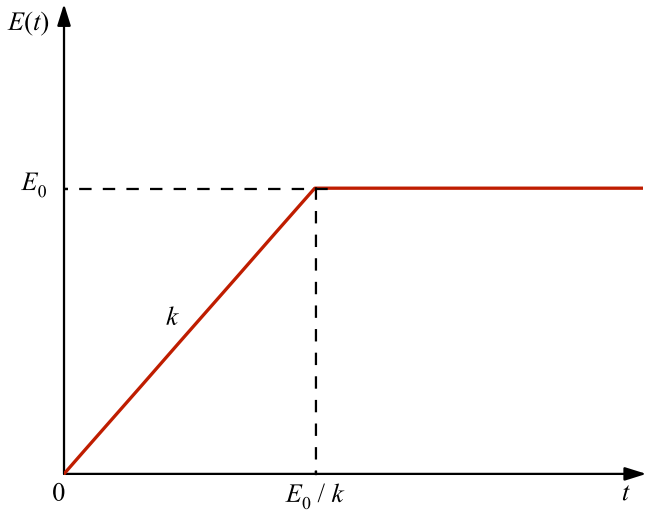

FIGURE 11 Electric field of charged molecules during vibration.

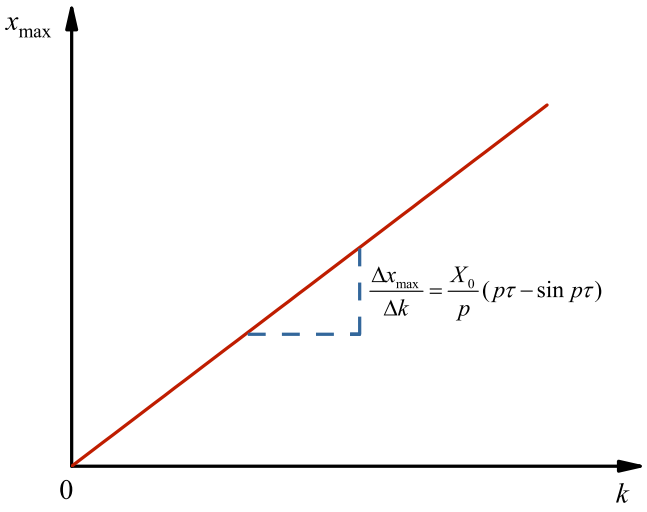

FIGURE 12 Amplitude of the vibrations against the rise time.

As per the previous analysis, the electric field acted on the excitation of the charged molecules for a very short time and only after a sudden change in the electric field, owing to the rapid response of the molecules. In addition, the electric field does not reach a steady state. However, the action time of an electric field is affected by many factors and it is difficult to calculate a specific value. Hence, this study aimed to deduce the motion relationships of charged molecules under a ramp-step electric field as a preliminary step. Therefore, it is assumed that the action time of the electric field is a constant that is significantly less than the change time of the electric field. If the action time of the electric field is τ ($\tau << E_0/k$), then the maximum value of the response can be expressed as

$$x_{\max} = \frac{kX_0}{p}(p\tau - \sin p\tau), \tag{6}$$

where X_0, p, and τ are constants.

As shown in Figure 12, the maximum response $x_{\max}$ is proportional to the slope of the electric-field edge k. Comparing the theoretical results in Figure 12 with the experimental results in Figure 6 shows that they are consistent, which proves the accuracy of the derivation process.

5 | DISCUSSION

The insulation failure mechanism caused by the pulsed electric field is shown in Figure 13. Owing to the effects of production processes and operating conditions, insulating materials contain defects such as bubbles and broken chains. Thus, free charges generated by electrode injections and impurity decompositions migrate to the vicinity of the defects where they are captured to form a space charge. In practical engineering applications, the intensity of the electric field in high-voltage power electronic devices can reach 30 kV/mm [30]. However, owing to distortion, the electric field intensity at the defect can be even higher. Such high-strength electric fields cause significant charge accumulation at the defect, which creates significant distortion in the electric field that can destroy the microstructure of the molecule.

The amplitude of molecular vibrations is proportional to the square of the electric-field intensity. Therefore, distortion of the field excites the molecular vibrations and significantly increases their amplitude. As they vibrate, molecular chains produce violently changing mechanical stresses. The defect-disposal subchain is relatively weak and under long-term, high-frequency, and high-strength electromechanical stress, the insulation defects gradually expand to form cracks and pores. As defects accumulate and the defect density increases, partial discharges and the initiation of electrical trees can occur, leading to insulation failure.

In summary, the mechanical stress caused by a pulsed electric field is an important factor in the early failure of insulators. Owing to the operating conditions of the equipment, it is difficult to reduce the mechanical stress by changing parameters such as the size and rate of change of the electric field force. However, the microstructure of insulating materials can be controlled via nanodoping and modification, and the material stress characteristics can be adjusted by changing the charge behaviour. Without reducing the insulation performance, the charge-relaxation time of the insulator may be reduced such that the material stress can keep up with the rate of change of the nanosecond-pulsed electric-field force. This would reduce the magnitude of the resultant force on the charged molecules at the pulse edges, thereby increasing the life of the insulator under a pulsed electric field.

6 | CONCLUSION

In this study, the relationship between the amplitude of the molecular vibrations, pulse parameters (edge time, edge slope, and voltage amplitude), and space charge density in a silicone

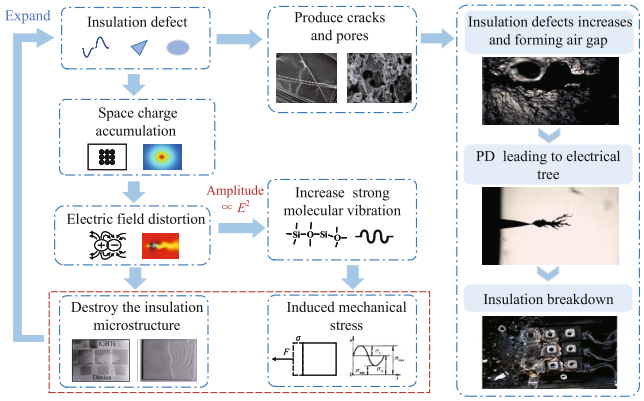

FIGURE 13 Mechanism of insulation damage under a pulsed electric field.

elastomer was explored by constructing a platform to simultaneously monitor the charge distribution and molecular vibrations. In addition, a mathematical model was established to investigate the dynamic process through which the molecular vibrations were induced by the pulsed voltage. The main conclusions are as follows.

(1) When a square-wave pulsed electric field with an edge time of microseconds to nanoseconds was applied to the silicone elastomer, the edge of the pulse stimulated the space charge inside the sample which drove molecular vibrations and generated sound waves. The amplitude of the molecular vibrations decreased sharply as the pulse-edge time increased, and it increased linearly as the pulse-edge slope increased. Moreover, the amplitude of the vibrations was proportional to the square of the amplitude of the pulsed electric field. Furthermore, the amplitude of the vibrations increased as the space charge density in the sample increased.

(2) Owing to the sudden change in the electric-field force at the pulse edge, the balanced forces on the charged molecules were disrupted, which caused them to vibrate under the action of a large resultant force. Thus, a mathematical model of molecular vibrations was established based on the spring-oscillator model. The excitation electric field at the rising edge of the pulse is equivalent to a ramp-step function; hence, the force inside the material is equivalent to a first-order elastic recovery force and the effects of resistance are ignored. A dynamic equation for the charged molecules at the pulse edge was also proposed. The equation was analysed and solved; thus, the mathematical relationship between the molecular-vibration amplitude and pulsed voltage slope was determined. Finally, a comparison of the theoretical and experimental results showed that they were consistent.

(3) Electrically induced mechanical stress is an important factor in the early failure of insulators. The accumulation of space charges at the insulation defect leads to distortion of the electric field. These distortions significantly increase the amplitude of the molecular vibrations and strong mechanical stresses occur at the defects, which expand to form pores. Furthermore, partial discharges occur in the pores, which lead to branching and insulation failure. Therefore, it is necessary to develop appropriate measures, such as doping with nanofillers, that can suppress the electromechanical stress and improve the reliability of power electronic devices under nanosecond-pulsed electric fields.

ACKNOWLEDGEMENTS

This research was financed by the National Natural Science Foundation of China (Grant Nos. 51907105 and 52277155).

CONFLICT OF INTEREST STATEMENT

The authors declare no conflict of interest.

DATA AVAILABILITY STATEMENT

The data that support the findings of this study are available from the corresponding author upon reasonable request.

ORCID

Junyu Wei https://orcid.org/0000-0002-4391-4983
Dongxin He https://orcid.org/0000-0001-8387-3146
Teng Gao https://orcid.org/0000-0002-7909-6927

REFERENCES

1. Ghassemi, M.: PD measurements, failure analysis, and control in high-power IGBT modules. High Volt. 3(3), 170–178 (2018)
2. Huang, M., et al.: Overview of recent progress in condition monitoring for insulated gate bipolar transistor modules: detection, estimation, and prediction. High Volt. 6(6), 967–977 (2021)
3. Locatelli, M.L., et al.: Evaluation of encapsulation materials for high-temperature power device packaging. IEEE Trans. Power Electron. 29(5), 2281–2288 (2014)
4. Ghassemi, M.: Accelerated insulation aging due to fast, repetitive voltages: a review identifying challenges and future research needs. IEEE Trans. Dielectr. Electr. Insul. 26(5), 1558–1568 (2019)
5. Wang, Y.L., et al.: Effect of micro and nano-size boron nitride and silicon carbide on thermal properties and partial discharge resistance of silicone elastomer composite. IEEE Trans. Dielectr. Electr. Insul. 27(2), 377–385 (2020)
6. Mancinelli, P., et al.: Analysis of electrical tree inception in silicone gels. IEEE Trans. Dielectr. Electr. Insul. 24(6), 3974–3984 (2017)
7. Wang, P., et al.: Effect of rise time on PD pulse features under repetitive square wave voltages. IEEE Trans. Dielectr. Electr. Insul. 20(1), 245–254 (2013)
8. Wang, P., Montanari, G.C., Cavallini, A.: Partial discharge phenomenology and induced aging behavior in rotating machines controlled by power electronics. IEEE Trans. Ind. Electron. 61(12), 7105–7112 (2014)
9. Zhao, L., et al.: An investigation into the cumulative breakdown process of polymethylmethacrylate in quasi-uniform electric field under nanosecond pulses. Phys. Plasmas 20(8), 082119 (2013)
10. Cavallini, A.: Reliability of low voltage inverter-fed motors at have we learned, perspectives, open points. In: International Symposium on Electrical Insulating Materials (ISEIM), pp. 13–22. Toyohashi, Japan (2017)
11. Wang, P., et al.: Effect of repetitive impulsive voltage duty cycle on partial discharge features and insulation endurance of enameled wires for inverter-fed low voltage machines. IEEE Trans. Ind. Electron. 24(4), 2123–2131 (2017)
12. Luan, C.B., et al.: All solid-state electromagnetic pulse simulator based on the 4H-SiC photoconductive semiconductor switch. Rev. Sci. Instrum. 91(1), 014701 (2020)

13. Zhang, B.Y., Ghassemi, M., Zhang, Y.: Insulation materials and systems for power electronics modules: a review identifying challenges and future research needs. IEEE Trans. Dielectr. Electr. Insul. 28(1), 290–302 (2021)
14. Wu, S.L., et al.: Effect of surface modification of electrodes on charge injection and dielectric characteristics of propylene carbonate. High Volt. 5(1), 15–23 (2020)
15. Su, J.G., et al.: Electrical tree degradation in high-voltage cable insulation: progress and challenges. High Volt. 5(4), 353–364 (2020)
16. Zhao, X.F., et al.: Interfacial space charge characteristic of PPLP insulation for HVDC cables. High Volt. 5(5), 628–635 (2020)
17. Akram, S., et al.: Charge transport and trapping of surface modified stator coil insulation of motors. IEEE Trans. Dielectr. Electr. Insul. 28(2), 719–726 (2021)
18. Xu, Z., et al.: Study on the influencing factors of space charge dynamic behavior in XLPE insulation under alternating current electric field. J. Phys. D Appl. Phys. 55(24), 245302 (2022)
19. Zhu, L.W., et al.: Electrical treeing initiation and breakdown phenomenon in polypropylene under DC and pulse combined voltages. IEEE Trans. Dielectr. Electr. Insul. 26(1), 202–210 (2019)
20. He, D.X., et al.: Space charge behaviors in cable insulation under a direct current-superimposed pulsed electric field. High Volt. 6(3), 426–434 (2021)
21. Takada, T., et al.: Determination of charge-trapping sites in saturated and aromatic polymers by quantum chemical calculation. IEEE Trans. Dielectr. Electr. Insul. 22(2), 1240–1249 (2015)
22. Zhang, Y.X., et al.: Electrical treeing behaviors in silicone rubber under an impulse voltage considering high temperature. Plasma Sci. Technol. 20(5), 054012 (2018)
23. Liu, X.Z., et al.: Electrical tree characteristics under AC and repetitive pulse voltages in wind turbine generator composite insulation. IEEE Trans. Dielectr. Electr. Insul. 27(3), 1007–1014 (2020)
24. Dai, C., et al.: Space charge dynamics in epoxy based composites under DC and square pulse wave of different polarities and frequencies. IEEE Trans. Dielectr. Electr. Insul. 28(6), 1980–1987 (2021)
25. Dai, C., et al.: Space-charge characteristics in epoxy composites under square pulse wave of different polarities with various frequencies at various temperatures. IEEE Trans. Dielectr. Electr. Insul. 29(1), 137–144 (2022)
26. Ren, H., Wang, J., Yan, P.: Study on electrical tree in PMMA under repetitive nanosecond pulses. Adv. Technol. Electral. Eng. Energ. 27(4), 32–35+67 (2008). (in Chinese)
27. Maeno, T., et al.: Measurement of spatial charge-distribution in thick dielectrics using the pulsed electroacoustic method. IEEE Trans. Electr. Insul. 23(3), 433–439 (1988)
28. Zhang, T., et al.: Charge vibration behaviour in polyimide under the pulse voltage with different rise and fall times. High Volt. 7(1), 64–74 (2022)
29. Li, Y., Yasuda, M., Takada, T.: Pulsed electroacoustic method for measurement of charge accumulation in solid dielectrics. IEEE Trans. Dielectr. Electr. Insul. 1(2), 188–195 (1994)
30. Li, K., et al.: Electric field mitigation in high-voltage high-power IGBT modules using nonlinear conductivity composites. IEEE Trans. Compon. Pack. Manuf. Technol. 11(11), 1844–1855 (2021)

How to cite this article: Wei, J., et al.: Behaviour and mechanisms of molecular vibrations induced by a pulsed voltage in a silicone elastomer used for device encapsulation. High Voltage. 8(5), 1020–1029 (2023). https://doi.org/10.1049/hve2.12363